INTELLIGENT DISTRIBUTION FAULT LOCATION USING VOLTAGE MAGNITUDE MEASUREMENTS

BY

SHAMINA SHAHRIN HOSSAIN

THESIS

Submitted in partial fulfillment of the requirements
for the degree of Master of Science in Electrical and Computer Engineering
in the Graduate College of the
University of Illinois at Urbana-Champaign, 2014

Urbana, Illinois

Adviser:

Professor Thomas Overbye

ABSTRACT

In an effort to increase situational awareness in the electric power grid, distributed monitoring devices are being implemented. These sensors allow the capture of fast-sampled voltage data such as frequency, voltage magnitude, and voltage angle measurements in a low-cost, easily deployable manner. Traditional fault location methods use both current and voltage data. Voltage monitoring devices only collect voltage data, but these sensors can collect this data anywhere along the distribution lines. An intelligent, iterative simulation-based fault location method using only voltage measurements, from anywhere on the line, is proposed. This technique involves comparing a measured voltage profile of a specific fault type and phase with a calculated voltage profile obtained through simulation of such a fault occurring at various locations with a range of probable fault impedances in the system. The simulated locations are intelligently selected using the Golden section search technique. The best match is determined using the $L1$-norm. The algorithm is successfully demonstrated using a PowerWorld case study.

To Taylor, Ammu, Baba, Boru Apu, Wafiq, Giang Chau, Cinda, and Marv: thank you for all your love and support, and supply of good food.

ACKNOWLEDGMENTS

I am very grateful for the support of my adviser, Professor Thomas Overbye, and my research group for all their help and guidance in my work. Professor Hao Zhu also played an integral part in this endeavor, for which I am very thankful. I would also like to thank the Illinois Center for a Smarter Electric Grid (ICSEG) for their continued support in this research.

TABLE OF CONTENTS

LIST OF TABLES

LIST OF FIGURES

LIST OF ABBREVIATIONS

COM	Component Object Model
SimAuto	Simulation Automation Server
GSS	Golden Section Search

CHAPTER 1

INTRODUCTION

Methods for fast, accurate fault location are integral in sustaining safe, reliable, and efficient generation and distribution of electricity in the grid. Faults are frequent occurrences in power systems and can stem from a variety of causes including over-voltages, equipment malfunction, and severe weather. Pinpointing faults in a distribution system is a vital function for outage management, repair, and return of service, especially to ensure optimal reliability. After a fault occurs, protective relays placed at the ends of the faulted line sense the fault immediately and isolate the line by opening the associated circuit breakers. The relays sense the fault by detecting the overcurrents caused by it [7], [8]. This detection then signals the substation to perform fault investigation [9].

To restore service to this line or any other further remedial action, a fault location algorithm is necessary to identify where the fault occurred. Thus, both detection and location methods are required after the occurrence of a fault. Although there are many available fault location methods for transmission lines, they cannot often be easily applied to distribution systems. This can be attributed to the complexity of the lines and the lack of instrumentation. System buses form a sparsely connected grid with monitoring devices located at the substations in transmission systems. Distribution systems, however, are typically radial configurations stemming from the distribution substations. Distribution systems are usually only monitored at the substation end of the feeders [10].

This can be remedied with the recent advent of distributed voltage monitoring devices that can collect synchronous voltage phasor data from anywhere on the line - not limited to the ends of the feeder [11]. Devices for collecting localized voltage information are results of an effort to improve situational awareness. Such monitoring sensors allow for access to voltage information throughout the entire power grid and, thus, the ability to moni-

tor and analyze these measurements in near real-time [12]. Visualization of a system's response to disturbances can also be achieved with access to localized measurements. With this availability of fast-sampled voltage magnitude data from distributed voltage monitoring devices, a fault location algorithm can be implemented. This provides the opportunity for an efficient and low-cost method for distribution systems to be developed.

Access to widespread voltage magnitude data from distributed devices allows for a distribution fault location method utilizing only voltage information. Such a method could improve the computational burden of traditional means, as it would reduce the amount of data processed. It also makes use of the cost-efficient distributed voltage monitoring devices, which are more economical than traditional substation-end devices to both install and maintain.

An iterative, simulation-based fault location method is proposed utilizing only voltage data, with no knowledge of current measurements. This algorithm aims to make use of the newfound availability of distributed voltage data obtained from monitoring devices and, therefore, only concentrates on the use of voltage measurements. It uses the Golden section search technique to intelligently select fault locations and impedances to simulate and compare with a measured voltage profile from a known distribution network after a fault has occurred. The $L1$-norm criterion is employed to determine the best match between simulated and measured voltage profiles. The method background, details, and results are presented in the following chapters.

CHAPTER 2

LITERATURE REVIEW

Traditional methods for distribution fault location use both voltage and current measurements, even those more focused on voltage sags. When a fault occurs, characteristic voltage sags, or reduction in system voltages, arise dependent on the fault location and system topology. Thus, a particular fault will have a specific voltage profile. Lotfifard *et al.* [1] describes a fault location approach for distribution systems based on data gathered from meters installed at some points along a feeder, such as power quality meters. A simple model of the faulted network and location of the meter is shown in Figure 2.1. The source impedance is represented as Zs, impedance between meter and fault as Z, and fault resistance as Rf. The meter collects the voltage sag information.

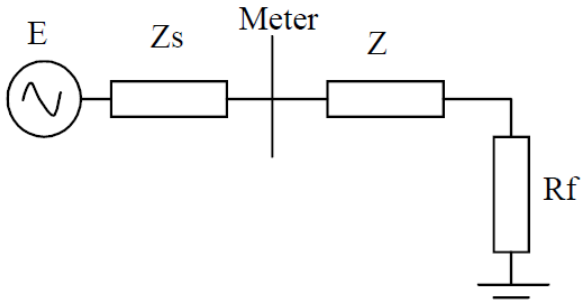

Figure 2.1: Model of faulted network with meter location collecting voltage sag information [1].

Knowledge of pre-fault and during-fault voltage and current phasors at the root node as well as information about the fault phase and type are required in this method. After the load models are updated using the pre-fault measurements, the during-fault current and voltage data is utilized to discover the fault location. Using the measured voltage sag data, a comparison is made with calculated voltage sags of faults at each node from a modeled network in a power flow program. The highest similarity is presumed to be

the location of the fault.

Li *et al.* [2] also present a fault location method for distribution systems using voltage sag measurements. This approach involves a power flow and fault analysis program, a database search method, and a pattern recognition technique to identify the fault section automatically. Figure 2.2 illustrates this process. However, information about fault current is still needed. Both methods require knowledge of pre-fault and during-fault currents in addition to voltages.

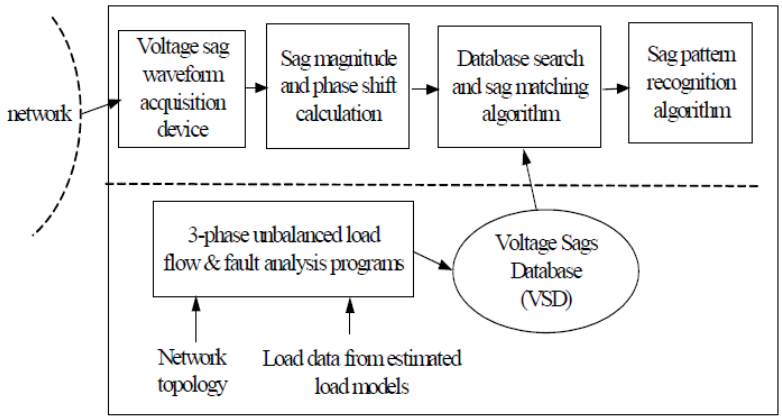

Figure 2.2: The proposed automatic fault section locator utilizing database search and pattern recognition techniques [2].

Another algorithm that utilizes voltage sag measurements was presented by Galijasevic *et al.* [3] and applies fuzzy logic reasoning techniques. Focused on transmission systems, the voltage data is measured at substation ends of the lines and subsequently compared with voltage sags calculated from fault simulations. The method utilizes the concept of vulnerability contours to assess the likelihood of voltage sags affecting a given network area in the transmission system. A vulnerability contour finds a circular area for fault locations where vulnerable or "bad" voltage sags are created after a fault, as shown in Figure 2.3. In this manner, the most likely location areas are found. Fuzzy logic is employed to address measurement uncertainties and, thus, enhance the estimation procedure. Such a technique is used when there is not enough information about a particular system to apply standard "yes/no" logic [3]. Nonetheless, the method is rather complex with its vulnerability contour and fuzzy logic steps. Also, as it is designed for transmission systems, locating a vulnerable area highlights the faulted bus as transmission networks

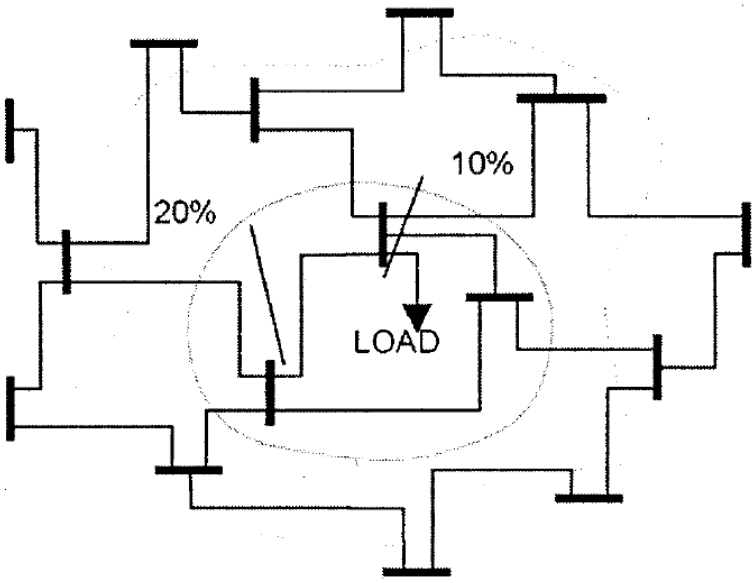

Figure 2.3: A short-circuit fault causes voltage sags of different levels at a load location [3].

are very broad and sparse. However, in a distribution system, the lines are closer together and the network is more populated. Thus, if the algorithm was translated to distribution systems, a vulnerable area may include many different buses. For proper maintenance and remedial actions, it is much more pertinent to find the faulted bus, rather than an area of many buses.

Taking advantage of smart feeder meters, Trindade *et al.* [13] utilize the distributed voltage sag measurements to estimate the fault location. However, this is achieved by "relating the voltage deviation measured by each meter to the fault current calculated based on the bus impedance matrix, considering the fault in different points" [13]. Therefore, the algorithm requires the analysis of both voltage and current.

However, with the availability of only voltage data from the distributed voltage monitoring devices – an algorithm using on voltage magnitudes is motivated. Now that these measurements are available, it is pertinent to use them to their fullest capability. If a fault location algorithm can be developed utilizing the expansive, fast-sampled voltage magnitude data, it must be explored as an alternative method for the future. By reducing the amount of parameters to analyze, the proposed algorithm will use solely voltage magnitude measurements to locate the fault location and its corre-

sponding impedance. Such an method will simplify the implementation and also take full advantage of the economical distributed voltage monitoring device capabilities.

CHAPTER 3

BACKGROUND

To augment the development of the fault location algorithm, background information on the tools and concepts utilized is presented below. As this is a distribution fault location method based on voltage sags, sections on distribution systems, faults, and voltage profiles are included. The manner by which the voltage profiles are compared is described in the cost function section and the search technique, by the Golden section search. Lastly, details on automation servers and their impact on the algorithm are given.

3.1 Distribution Systems

An electric power system, or power grid, is comprised of two major networks, the transmission system and the distribution system. After electricity is generated at power plants, the transmission network transports that power to load centers where it is then supplied to customers through the distribution system. This is illustrated in Figure 3.1. The transmission system functions to deliver the generated energy to the system, thus supplying the subtransmission and distribution networks. The three-phase transmission lines are rated at voltages ranging from 230 to 765 kV. Subtransmission systems step down this voltage via step-down transformers and connect to distribution networks. The distribution system subsequently steps down the voltages to 2.2 to 46 kV for local distribution [10].

Distributing energy from the distribution substations consists of primary and secondary distribution. Primary distribution carries energy from the distribution substations to the distribution transformers for the voltages to be stepped down for consumer levels. Secondary distribution, after voltages are stepped down, is where the energy is distributed to all the customers.

The distribution network, in primary distribution, consists of a three-phase

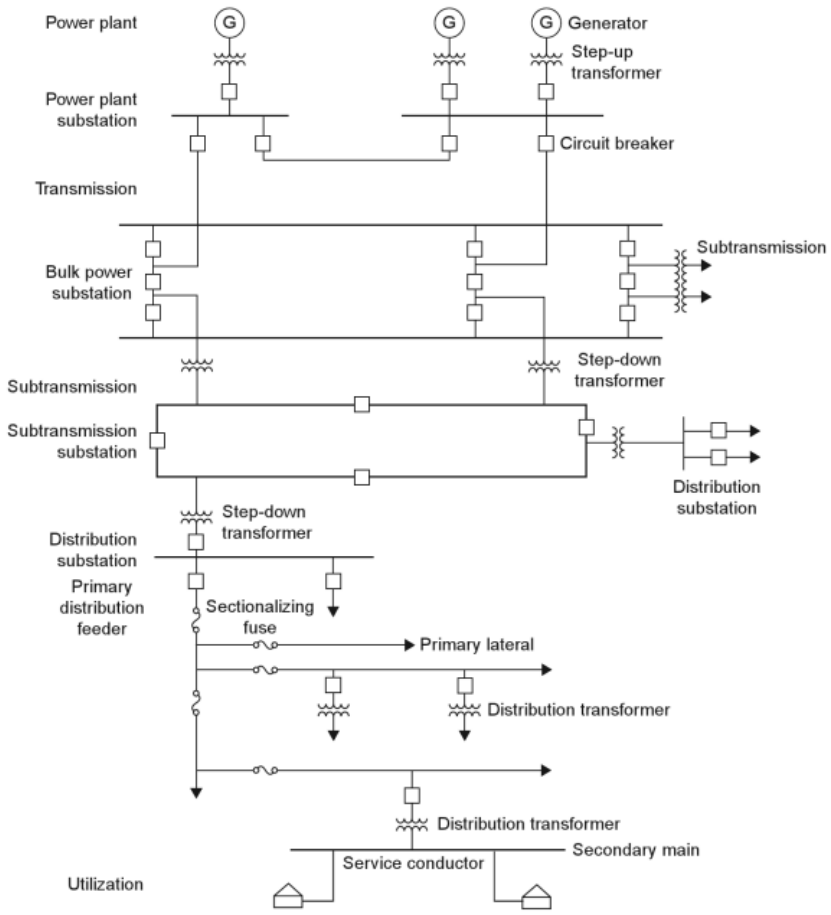

Figure 3.1: Basic electric power system [4].

system in which there are three basic configurations: radial, loop, and primary network systems. Simplified diagrams of these networks are shown in Figure 3.2, Figure 3.3, and Figure 3.4. Essentially, a radial system involves one power source for a group of customers while a loop system has an alternate source available. A primary network is an interlocked system with more than one source and is the most reliable, but also the most complex of the three [14].

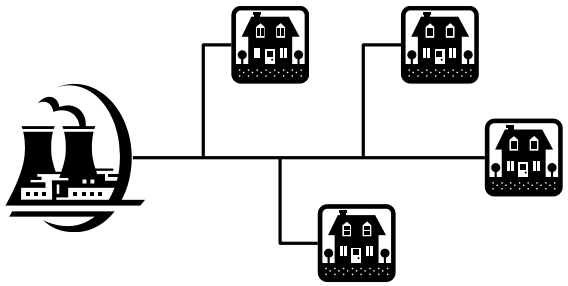

Figure 3.2: Radial configuration: one power source.

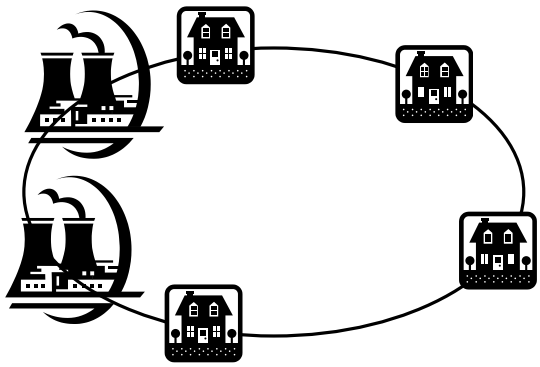

Figure 3.3: Primary loop configuration: alternate source exists.

Radial systems are the most commonly used configurations and will be the focus of this work [10]. Three-phase feeders stem from a distribution substation in a radial manner, as shown in the more detailed configuration in Figure 3.5. Since a radial system consists of one power source for a group

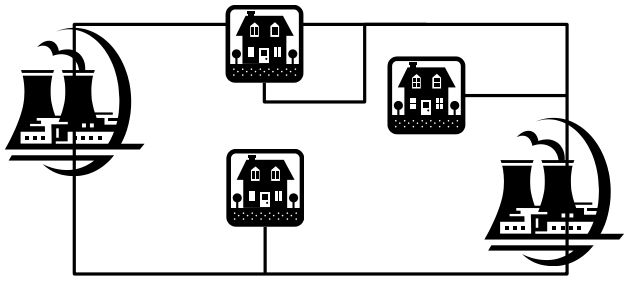

Figure 3.4: Network configuration: interlocking, reliable.

of customers, a fault would interrupt power in the entire line and create a characteristic voltage profile. Such voltage profiles and faults are discussed in the subsequent sections.

3.2 Faults

When a circumstance arises that interferes with the normal flow of current in the power system, a fault has occurred. This sudden condition could stem from events such as severe weather or equipment damage to even a tree branch making contact with a line. The fault current, or resulting short circuit, is dependent on internal voltages of the machines and system impedance between the machines and the location of the fault [10]. These currents can reach very high magnitudes, in comparison to normal system current levels, and can cause severe damage to network components. Therefore, it is pertinent to locate and clear these faults promptly. There are four main types of faults that can occur in a three-phase system, listed and illustrated below in Figure 3.6, Figure 3.7, Figure 3.8, and Figure 3.9 :

1. Single-line-to-ground
2. Line-to-line
3. Double-line-to-ground
4. Balanced-three-phase fault

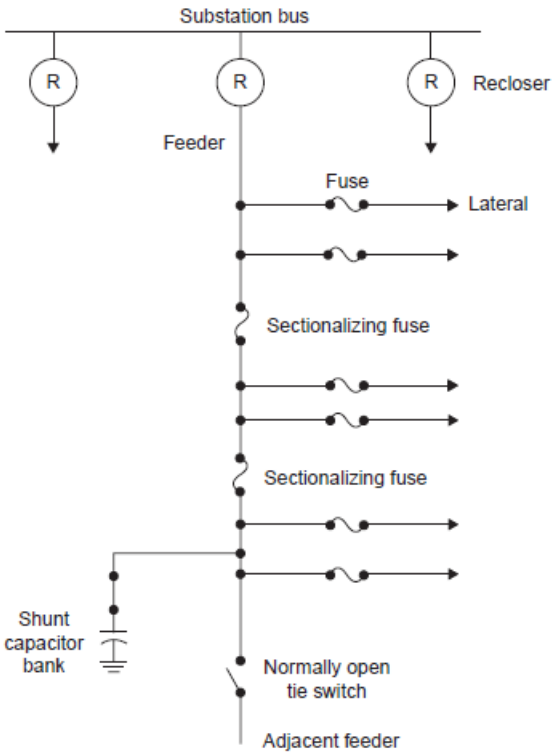

Figure 3.5: Radial distribution system configuration [4].

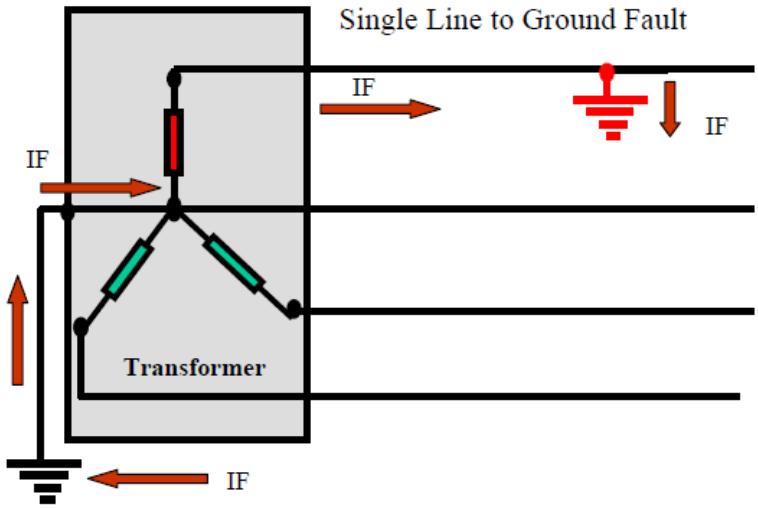

Figure 3.6: A single-line-to-ground fault where a short circuit is created between a line and ground [5].

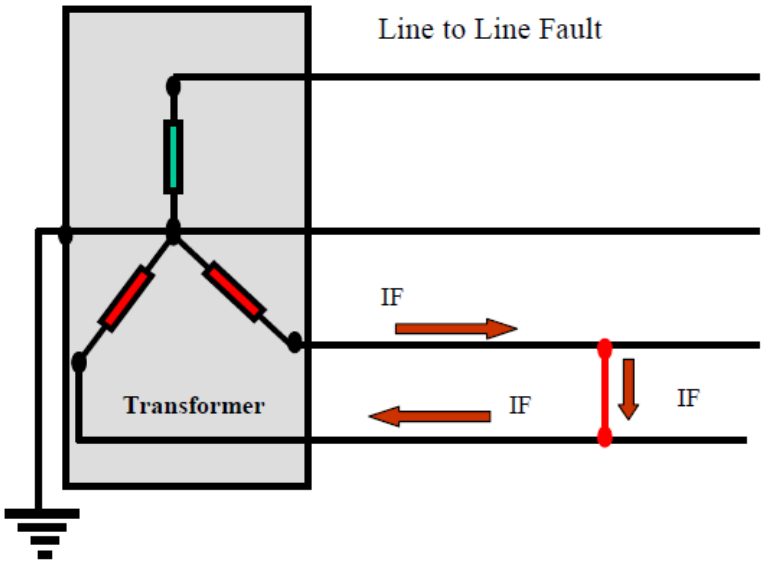

Figure 3.7: A line-to-line fault where a short circuit is created between two lines [5].

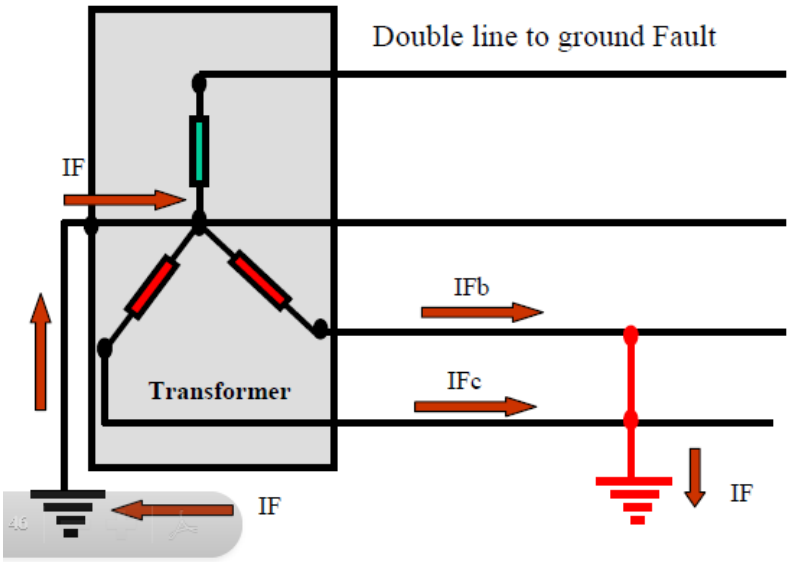

Figure 3.8: A double-line-to-ground fault where a short circuit is created between two lines and ground [5].

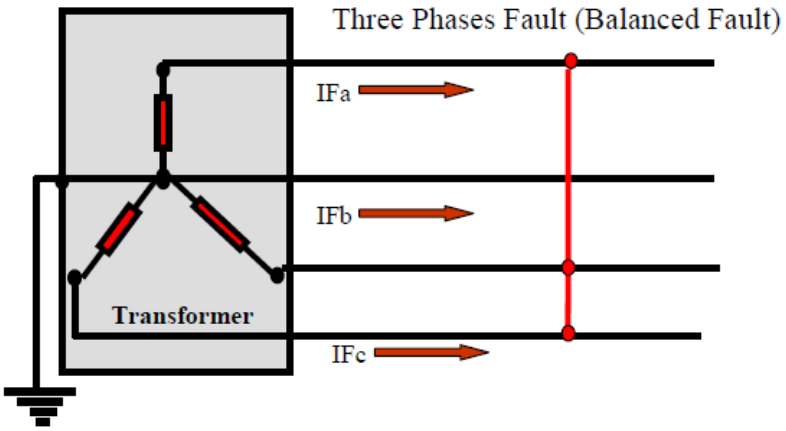

Figure 3.9: A balanced-three-phase fault where a short circuit is created on all three lines and affects all three phases equally [5].

Single-line-to-ground faults are the most common in power systems, as about 80% of faults in distribution systems are of this type [15]. In this type of fault, a short circuit is created between the line and ground, involving physical contact. Similarly, a double-line-to-ground fault is when two lines come in contact with the ground. This is often caused by lightning or storm damage. A line-to-line fault is when a short circuit occurs between two lines either from the ionization from the air between them or the fact they have come in contact. Faults $1-3$ are unsymmetric faults. When an unsymmetrical fault occurs in a balanced system, the sequence networks are only interconnected at the fault location [10]. Balanced three-phase faults are when a short circuit is created on all three lines and affects all three phases equally. This type of symmetric fault is simplest to analyze and is chosen to be initially studied for this project. Essentially, a symmetrical fault affects all phases equally and an unsymmetrical fault does not, removing the assumption that the current magnitude in all phases are equal.

Nevertheless, the detection of these various faults in the grid is a major objective for sustaining safe, reliable, and efficient generation and distribution of electricity in the power system. Thus, fault location algorithms are crucial for quick, remedial actions to be taken in order to prevent costly aftermath.

3.3 Localized Measurements and Voltage Profiles

When a fault occurs, characteristic voltage sags, or reduction in system voltages, arise depending on the fault location and system topology [3]. Thus, a particular fault will have a specific voltage profile, as obtained from the recent advent of distributed monitoring devices. Such devices offer the availability of localized measurements throughout the grid and are results of an effort to improve situational awareness. These devices can collect synchronous voltage phasor data from anywhere on the line – not limited to the ends of the feeder. Such monitoring sensors allow for access to voltage information throughout the entire power grid and, thus, the ability to monitor and analyze these measurements in near real-time.

With access to the voltage profile of a system after a fault occurs, the characteristic response can be studied to pinpoint the location and impedance of the fault incurred. An example profile after a fault is shown in Figure 3.10, where a fault has occurred at Bus 4 with an impedance of 5Ω.

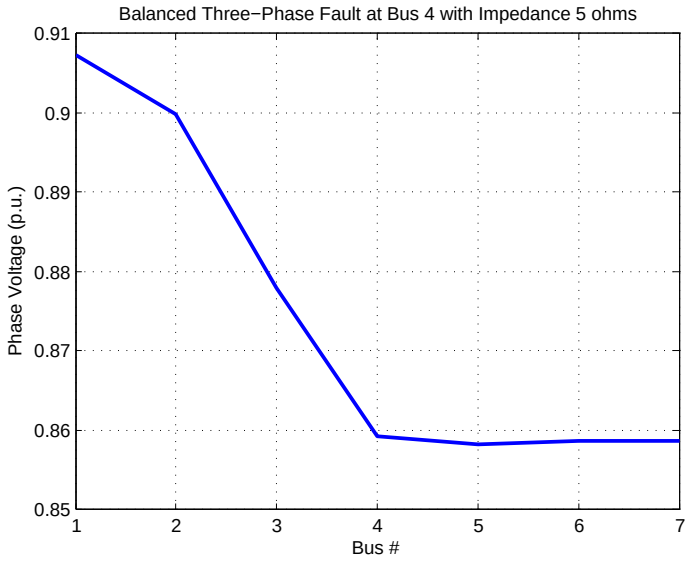

Figure 3.10: Voltage profile after a balanced three-phase fault at Bus 4 with an impedance of 5Ω occurred in a 7-bus radial system.

3.4 Cost Function

For voltage profiles or any two vectors to be numerically compared, cost functions are often employed. A cost function is a real number measure that intuitively represents a "cost" between one or more variables after some event [16]. In this case, if the cost function between two voltage profiles is the difference, we seek to minimize it to find the best match. Therefore, a suitable cost function is the $L1$- or *One* Norm. Given the two voltage profiles in Figure 3.11, the $L1$-Norm is the sum of the absolute values of the columns, as shown [16].

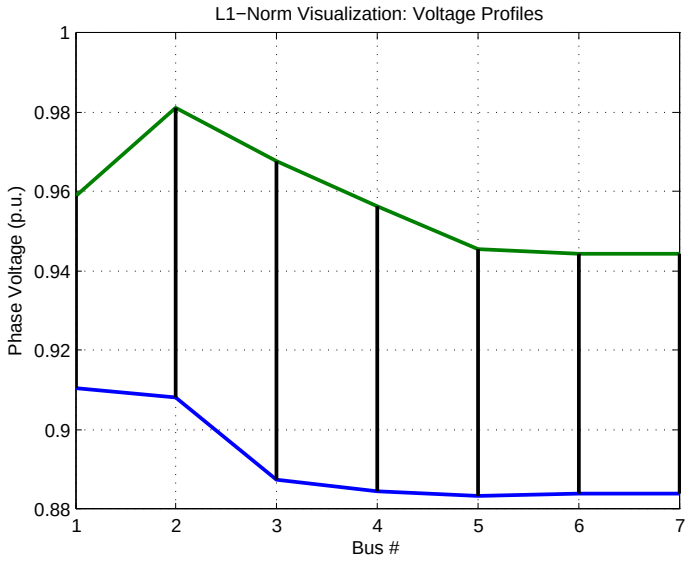

Figure 3.11: Voltage profile after a balanced three-phase fault at Bus 4 with an impedance of 5Ω occurred in a 7-bus radial system.

Mathematically, this is written as:

$$y = [y_1 \ y_2 ... y_n]^T \tag{3.1}$$

$$\hat{y} = [\hat{y}_1 \ \hat{y}_2 ... \hat{y}_n]^T \tag{3.2}$$

$$d = ||y\_\hat{y}||_1 = \sum_{i=1}^{n} |y_i - \hat{y}_i| \tag{3.3}$$

The variable d_i is the result of the evaluation of the $L1$-Norm between two vectors or profiles, y and $\hat{y}$. In this manner, the smallest difference between two vectors can be found and used to determine the best match.

3.5 Golden Section Search

The Golden section search is a technique for finding an extreme minimum or maximum by successively narrowing down a range in which the extremum is known to exist [16]. After establishing the start and end point of a range, it determines probing points according to the golden ratio, $\phi = \frac{1+\sqrt{5}}{2} = 1.618033...$ The benefit of using the golden ratio is that efficient search algorithms reduce the range by the same fraction in every iteration, which can be achieved using the golden ratio. Figure 3.12 shows range start and end points x_1 and x_3 and probing points x_2 and x_4.

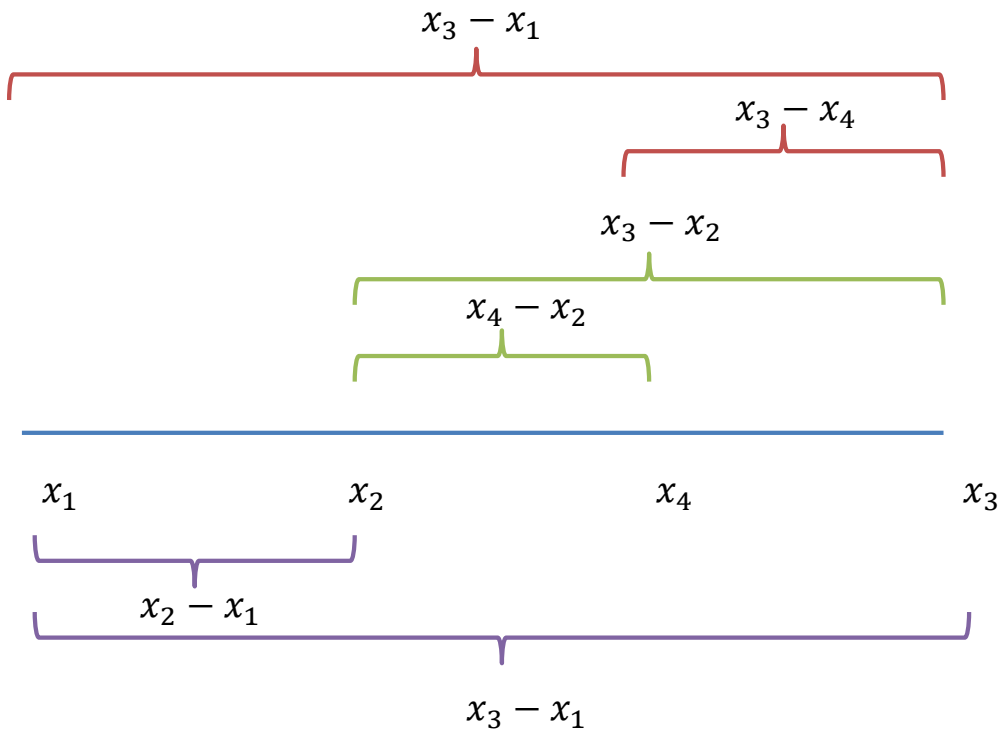

Figure 3.12: The ratios of the colored brackets must be equal for the method to reduce range by same fraction in every iteration.

The ratio of intervals, signified by the colored brackets, must be the same.

The required relationships are shown below.

$$x_2 - x_1 = x_3 - x_4 \tag{3.4}$$

$$\frac{x_2 - x_1}{x_3 - x_1} = \frac{x_4 - x_2}{x_3 - x_2} \tag{3.5}$$

Solving these relationships for the probing points results in:

$$\frac{x_4}{x_2} = \frac{1 + \sqrt{5}}{2} = 1.618033... \tag{3.6}$$

Therefore, the two relations specified guarantee that no matter which bound is discarded, the same fraction of the interval is eliminated. This is the motivation for utilizing the golden ratio in this search technique.

Returning to the algorithm process, the evaluation of the function at the probing points is used to narrow down the range in each iteration. The technique maintains the function values for triplets of points whose distances form the golden ratio. This search algorithm only works with strictly unimodal functions where the function $f(x)$, for some value m, is monotonically decreasing for $x \leq m$ and monotonically increasing for $x \geq m$, or vice versa. A typical stopping criterion is when given range start and end points x_1 and x_3 and probing points x_2 and x_4:

$$|x_3 - x_1| < \tau(|x_2| + |x_4|) \tag{3.7}$$

This process is exemplified in Figure 3.13 (a)-(d). The search algorithm begins in (a) and successively narrows down the range until the stopping condition is satisfied in (d).

Some of the benefits in using this search routine are:

1. It is robust and can handle any strictly unimodal function.
2. After the initial iteration, only one new probing point needs to be evaluated every iteration– reducing the amount of evaluations needed.
3. Convergence guaranteed – can handle poorly conditioned problems.
4. Reduces interval by same fraction in every interval for efficient search.
5. No derivatives needed; simple to implement.

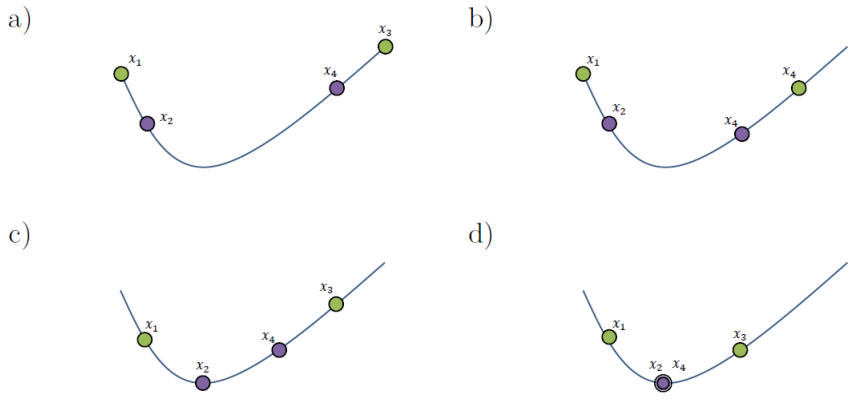

Figure 3.13: Golden section search example in which the minimum of the unimodal function is iteratively found.

Some disadvantages include that two initial guesses are required when beginning the algorithm and that it does not have as fast convergence rate as other existing search algorithms. The number of iterations necessary is dependent on a particular tolerance, ϵ, as specified by the user. The total number of function calls, N, needed for convergence is:

$$N = \frac{ln(\epsilon)}{ln(1-\tau)} + 3 \tag{3.8}$$

where $\tau = 0.38197$, from the golden ratio derivation. Nonetheless, implementation is relatively straightforward, making Golden section search an favorable tool for the initial development of a comparison-based fault location algorithm.

3.6 Automation Server

Power system analyses often require using a power system simulation software as well as external processing of the results in a separate computational program. This research utilizes the fault analysis tool of PowerWorld, a commercial simulation software, and Matlab for the additional calculations. Since the proposed algorithm is simulation-based, many simulations must be performed and the subsequent results have to be transferred to Matlab.

This requires importing and managing the resulting data into the external platform, increasing user effort and rendering the process quite cumbersome [17]. This is shown in Figure 3.14. One of the capabilities of commercial

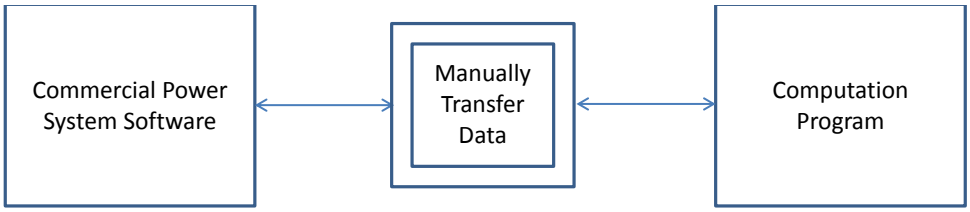

Figure 3.14: Required data transfer between simulation and computational platforms.

software such as PowerWorld is an Component Object Model (COM) automation server which allows the software to be directly interfaced with an external processing program [18]. This enables automatic retrieval of data without needing to maintain a database manually. This automation would allow for a more straightforward algorithm and freedom in the design.

A COM automation server is a binary-interface standard for software components; automation allows an application to manipulate objects implemented in another application, or to expose objects so they can be manipulated [19]. Thus, it allows objects to be reused without knowledge of the manner in which they were internally implemented, in any language – creating interfaces that are largely implementation independent, as shown in Figure 3.15.

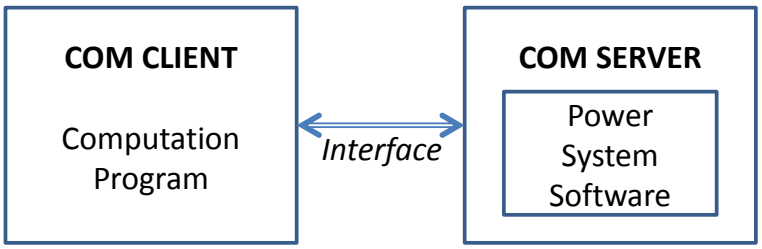

Figure 3.15: Interface between computation program and power system software using a COM automation server.

The Simulation Automation Server (SimAuto) of PowerWorld is a COM automation server [18]. It provides users the ability to externally access the functionalities of PowerWorld Simulator from within a program that was

externally built. This is achieved through simulator script commands utilized in an external environment [20]. This interface between the two programs eliminates manually retrieving and transferring data from PowerWorld to Matlab. It allows for a more straightforward implementation in which many simulations and the subsequent processing can be done with ease, as the burdensome steps are now automated. This process is shown in Figure 3.16.

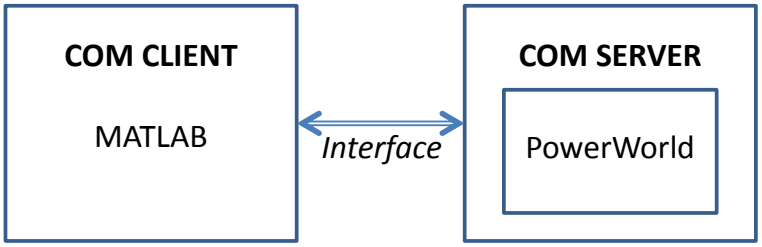

Figure 3.16: Interface between Matlab and PowerWorld using a COM automation server.

The use of automation servers between commercial power system software and external computation programs is a beneficial tool in the development of precise and effective algorithms and analyses. The automatic transfer of data between the two platforms eliminates the need to maintain databases manually and streamlines processing. Utilizing the COM automation server, a capability of most commercial power system software, enables greater freedom in the design of data-driven methods and removes cumbersome steps. It also allows information about how the system behaves , i.e. contour plots, to be acquired easily as such plots would be very burdensome to generate without automation. Without the use of SimAuto, this research would require much more manual work in terms of data storage and switching back and forth between the computation and power system simulation platforms [21].

CHAPTER 4

METHOD

Given a fault of known type and phase has occurred in the distribution system, a voltage profile of the network is received from the distributed monitoring devices. The measured voltage profile, along with the fault type and phase, are inputs for the fault location algorithm. The model of the particular distribution system is also available. A simplified diagram is shown in Figure 4.1 of the method's goal.

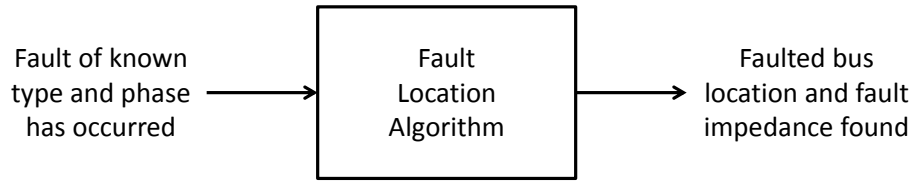

Figure 4.1: The final output of the algorithm is the faulted bus location and the associated fault impedance.

The algorithm subsequently obtains the voltage profiles for the initial locations as selected by the Golden section search (GSS). The fault at the initial bus locations are iterated through with all possible impedance values. Each combination's resulting voltage profile is compared with the measured voltage profile using the $L1$-norm, the cost function. For each of the initial bus locations, the impedance that provides the minimum $L1$-norm is chosen as the most likely combination for that particular bus location.

The four resulting bus location and best match impedance results are then compared against one another using the conditions of the GSS. Thus, if convergence or satisfaction of the stopping criteria is not achieved, new bus locations are selected and the process is repeated. If convergence is obtained, the best match fault location including bus number and fault impedance has been found. This process is illustrated in Figure 4.2.

Essentially, the algorithm will behave as follows:

1. Obtain measured voltage profile from system.

2. Apply the Golden section search to select the range and probe locations according to $L1$-norm error values between selected and measured voltage profiles.

    - Call power simulation software to simulate faults at selected locations with range of impedance values.
    - In a computation platform, calculate the $L1$-norm error between the measured and each of the simulated profiles. Apply search routine according to least error – the bus location and impedance value combinations that give the minimum $L1$-norm result.

3. Search routine converges on the best match fault bus location and impedance or terminates when norm is under specified threshold value.

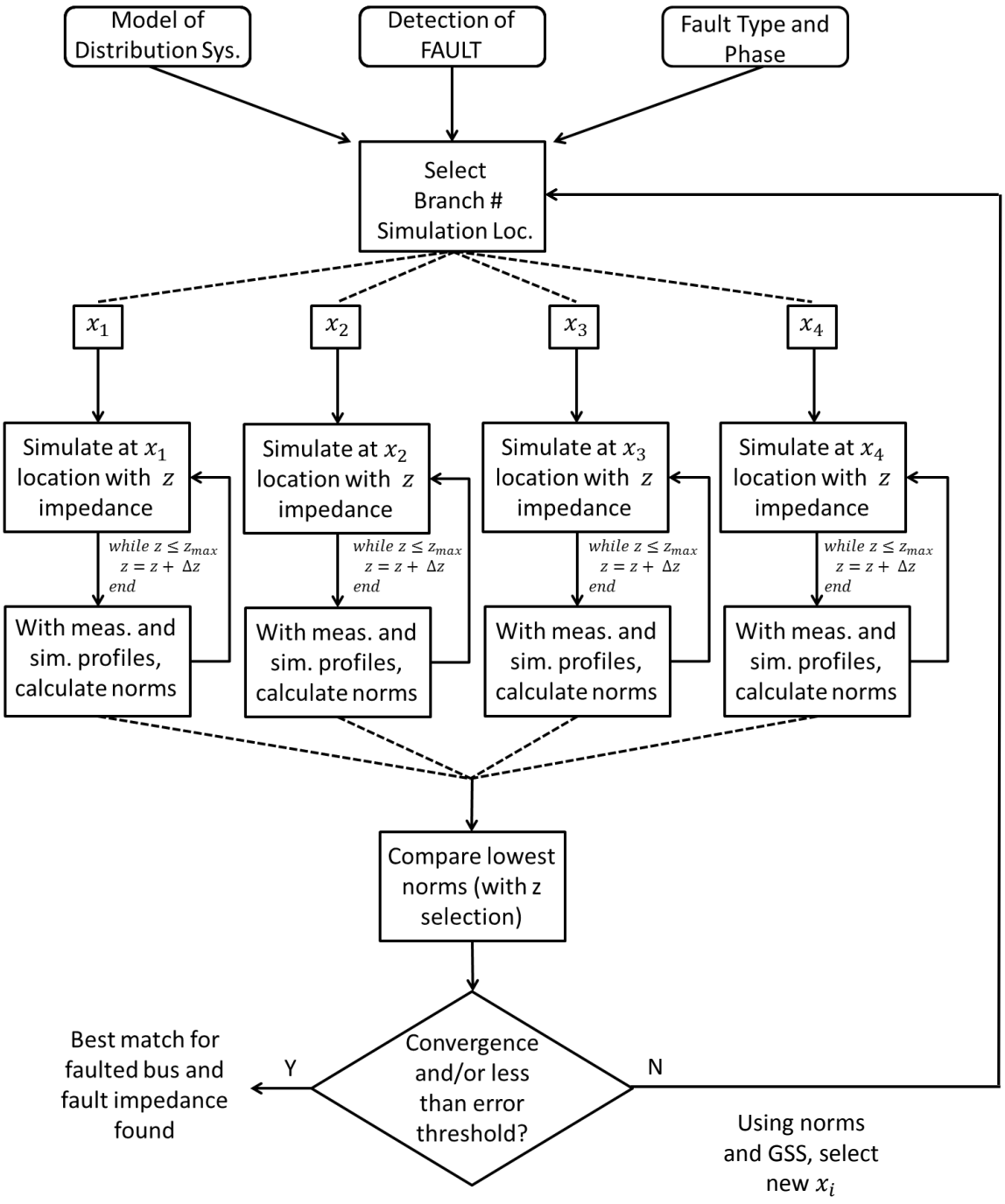

Figure 4.2: Process of the fault location algorithm.

CHAPTER 5

CASE STUDY

5.1 Setup

To demonstrate the use of the method, a 13-bus PowerWorld case, in Figure 5.1, is utilized. The feeder system is comprised of 13 buses and 10 loads that are classified as either primarily commercial, industrial, or residential [10]. As can be seen from the one-line diagram, the breaker between Bus 7

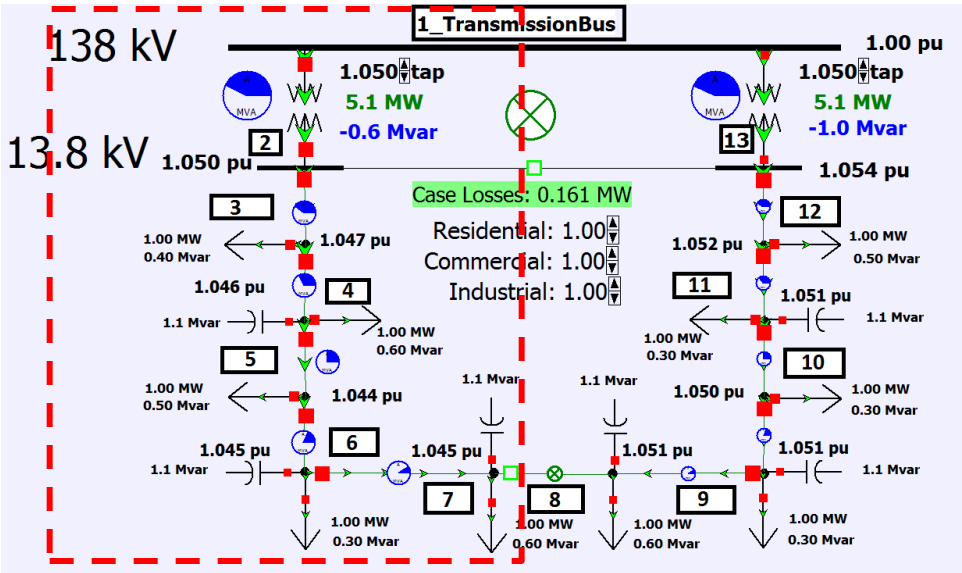

Figure 5.1: Feeder system in which Buses $1-7$ form a radial configuration.

and Bus 8 is open and, therefore, two separate radial systems are represented. For testing the algorithm, the radial system composed of Buses $1-7$ is used.

PowerWorld, a power system software, is employed for simulating the faults and obtaining voltage profiles. For the computational processing of the measured and simulated profiles, Matlab is utilized. SimAuto, the COM automation server of PowerWorld, is also used to streamline the algorithm and eliminate manual retrieval and storage steps.

5.2 Parameters

Since the model of the distribution system is given and known, the maximum impedance, threshold, and tolerance values are derived from an initial study. By studying typical fault currents, the maximum impedance of the system is calculated to be 60Ω. A conventional tolerance value of 0.01 is applied for terminating the algorithm if the best match is converged upon with the GSS conditions. If the error norm calculated in an iteration is already less than the threshold value, the best match has been found and the time required to check convergence can be avoided. The threshold value is derived from the study of contour plots of the error norms for a particular fault compared against all possible combinations of fault location and impedance, as shown in Figure 5.2 and Figure 5.3. The darkest color represents the area with the least norm error value.

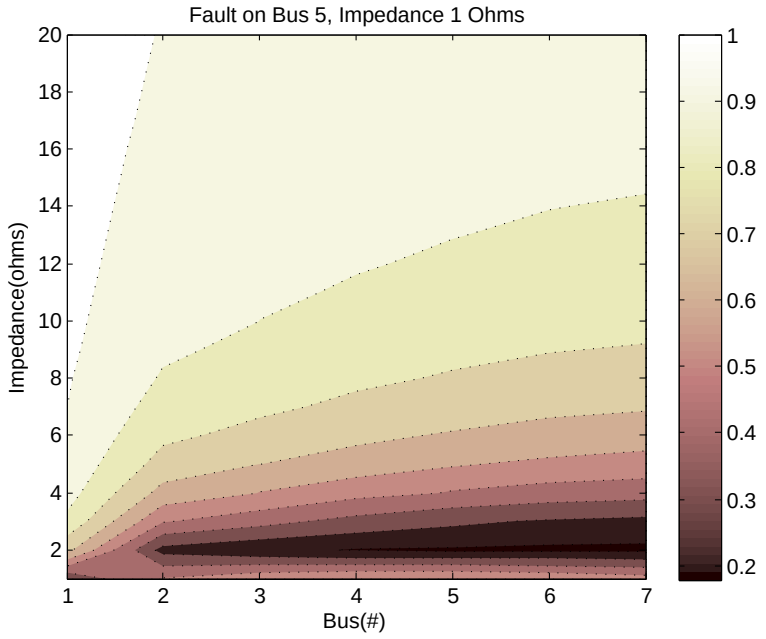

Figure 5.2: Simulated balanced three-phase fault on Bus 5 with Impedance 1 Ω compared with measured voltage profiles of every location and impedance combination.

By studying the contour plots and the average error norm of the correct bus location and impedance, accounting for noise, the threshold value is set to be 0.03; meaning, if the error norm is less than 0.03, the associated bus location and fault impedance is the most likely actual combination.

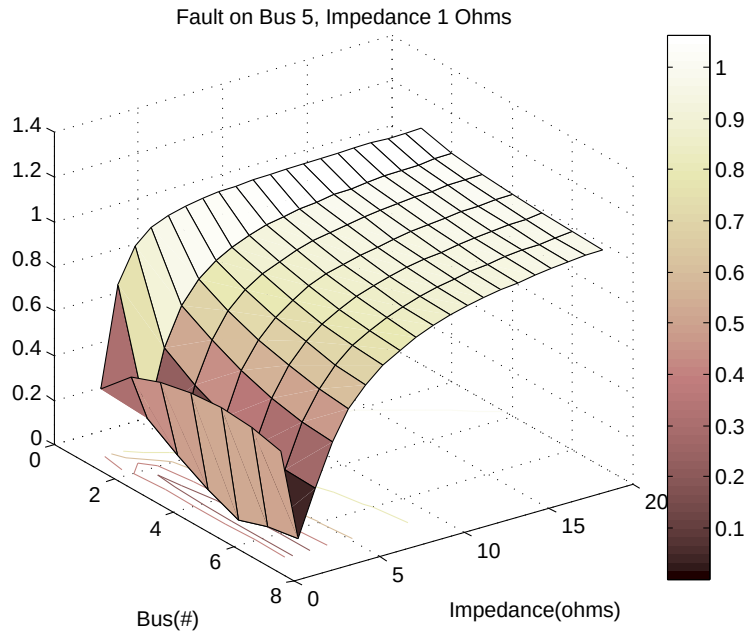

Figure 5.3: Surface contour plot of balanced three-phase fault on Bus 5 with Impedance 1 Ω compared with measured voltage profiles of every location and impedance combination.

Another insight to be gained from the contour plots is that the nature of the fault location problem is unimodal, as required by the Golden section search. This is more apparent in Figure 5.3, the surface contour plot, where the cost function decreases until the correct combination (the dip at Bus 5, Impedance 1Ω) and increases immediately after. This behavior allows the use of the Golden section search in finding the most minimum $L1$-Norm error, as to locate the faulted bus and fault impedance.

5.3 Pseudo-Measured Voltage Data

To emulate the measured voltage data obtained from the distribution network after a fault, a pseudo-measured voltage profile was created. A specific fault was simulated in PowerWorld and was subsequently processed in Matlab for the addition of noise. This noise was to mimic the highest measurement accuracy noise of the distributed voltage monitoring devices, which is usually 0.005 or 0.5%.

Thus, random noise was generated using Matlab's command for normally

distributed pseudorandom numbers. If m is the final measured data, s is the simulated, and n is the set of random noise, the final measured data is achieved as follows:

$$m = s + 0.005 \cdot n \tag{5.1}$$

In this manner, the measured voltage data encompasses the effect of measurement noise, imitating the realistic data from distributed devices. For this case study, the random noise set is kept constant as to pinpoint differences with different faults incurred not associated to noise.

5.4 Results

The fault location method was tested with an array of faults occurring in the 7-bus radial distribution system, including those listed in Table 5.1. Pseudo-measured voltage data was created for the listed combinations of fault location and fault impedance. Subsequently, it was inputted into the algorithm with known fault type and phase, as well as distribution model in PowerWorld. The fault type was balanced three-phase, affecting all phases equally. As observed in the table, the method was successfully able to find all the faults within 1 or 2 iterations and a maximum of approximately 22 seconds. The maximum variation was 5Ω for impedance, which is within range of reasonable difference. Figures 5.4-5.8 display the visual comparison of the actual and found fault voltage profiles, illustrating that the results were very closely matched. The maximum error difference between these profiles was 0.0219.

Table 5.1: Results of algorithm after various balanced three-phase faults have occurred in 7-bus radial system.

Actual Fault	Algorithm Result	Final Error	Iteration #	Time (s)
Bus 1, 13 Ω	Bus 1, 18 Ω	0.007	1	8.592064
Bus 3, 10 Ω	Bus 3, 10 Ω	0.0219	1	18.374962
Bus 4, 5 Ω	Bus 4, 5 Ω	0.0219	2	14.005770
Bus 6, 5 Ω	Bus 6, 5 Ω	0.0219	2	21.487154
Bus 7, 18 Ω	Bus 7, 19 Ω	0.0082	1	13.446661

All in all, the algorithm worked quite well in intelligently comparing the

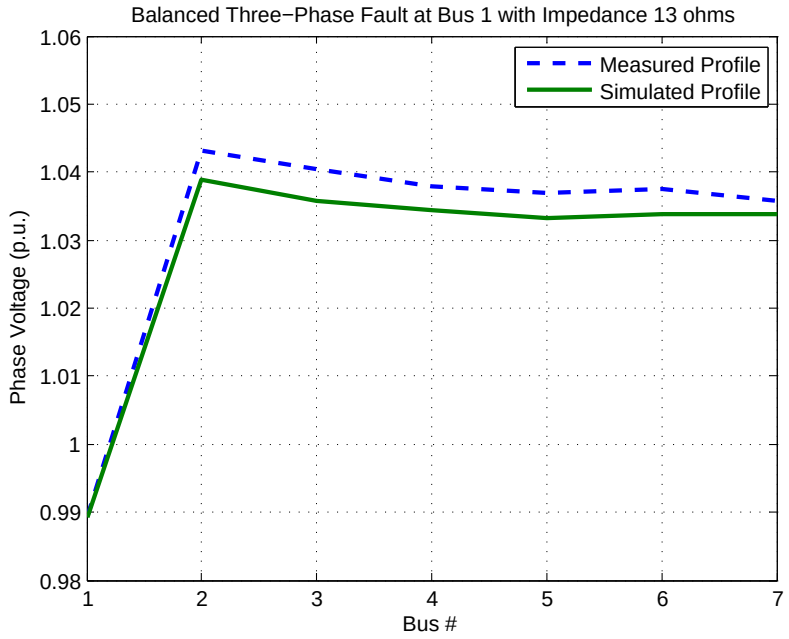

Figure 5.4: Comparison of best match calculated and measured profiles for a balanced three-phase fault at Bus 1 with Impedance of 13 Ω.

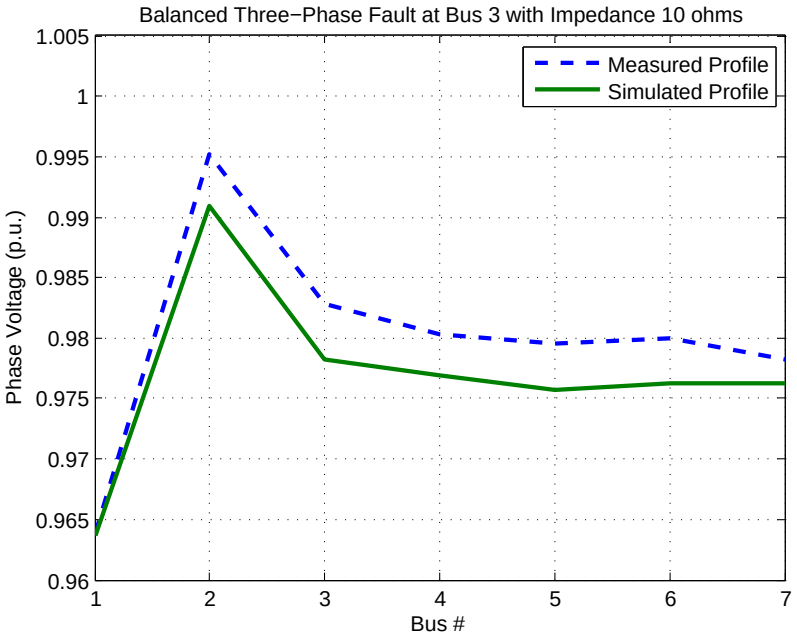

Figure 5.5: Comparison of best match calculated and measured profiles for a balanced three-phase fault at Bus 3 with Impedance of 10 Ω.

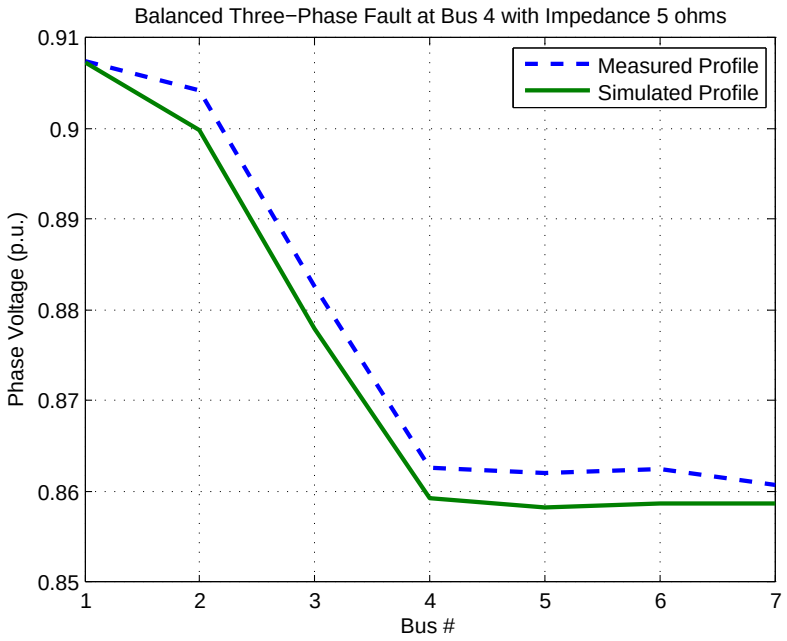

Figure 5.6: Comparison of best match calculated and measured profiles for a balanced three-phase fault at Bus 4 with Impedance of 5 Ω.

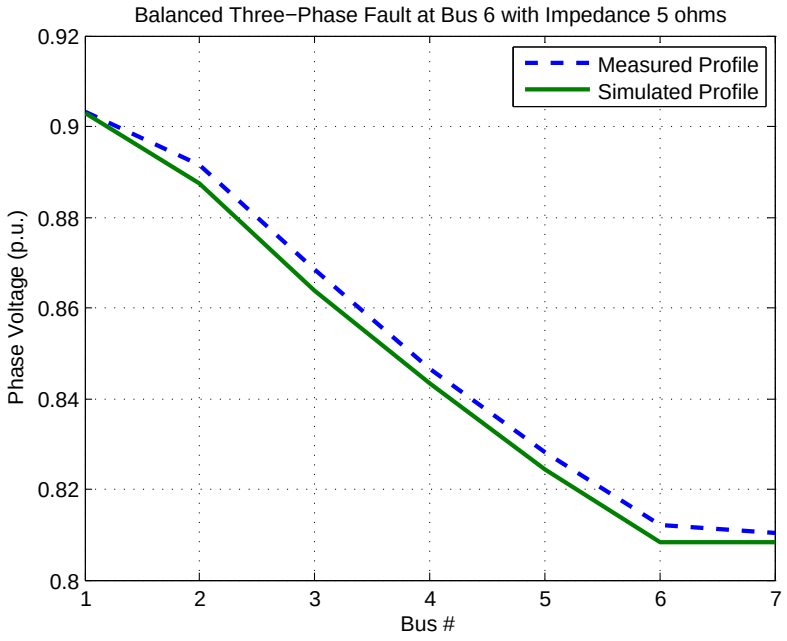

Figure 5.7: Comparison of best match calculated and measured profiles for a balanced three-phase fault at Bus 6 with Impedance of 5 Ω.

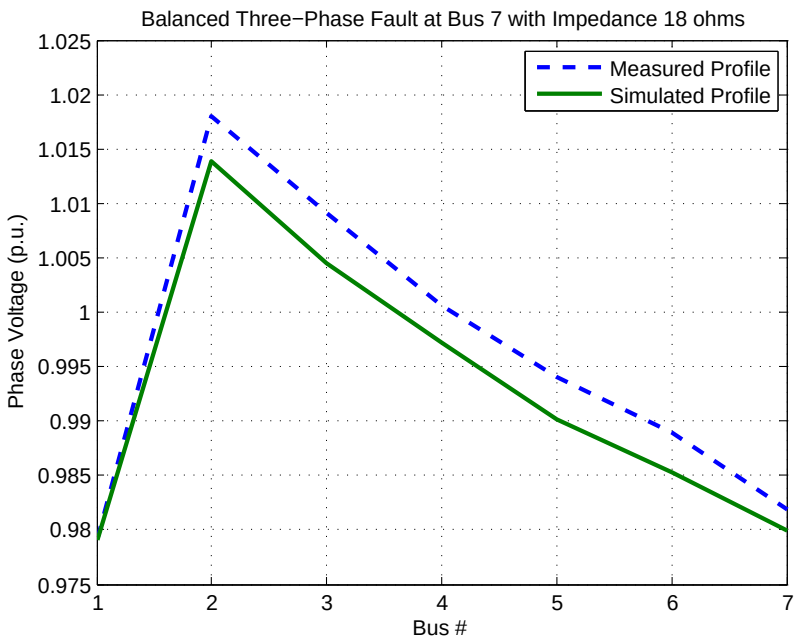

Figure 5.8: Comparison of best match calculated and measured profiles for a balanced three-phase fault at Bus 7 with Impedance of 18 Ω.

measured and simulated voltage profiles to obtain the best match fault location. The results indicate that future work can be done in perhaps reducing the impedance variation as demonstrated by the Bus 1, 13Ω fault and also reducing the run-time even further. It will be useful to test larger systems and observe if the run-time and iteration number still remains low.

CHAPTER 6

FUTURE WORK

As the results indicated in the previous section, there exists impedance variation between the actual and found faults. In the small case study presented, it is apparent that this variation is not excessive, as the largest difference was about 5Ω. It will be necessary to explore if this variation increases with different, larger systems. If it does, ways to reduce the difference in actual and found impedance will be studied.

To further improve the method, it will be explored if the exact location *along* the faulted can be identified. Presently, the algorithm locates the faulted bus and associated fault impedance. However, if it could output where along the line, such as at 25% or 60% of the line (where the start and end range of $0 - 100\%$ is pre-defined), the information would be even more powerful. This would allow service crews to have a more accurate description of where the fault occurred and, hopefully, more efficient and quick repairs.

This inclusion is currently being explored in this research, finding the exact % location along the faulted line. In this manner, the faulted line is defined as a branch – a line between two buses. An alternate algorithm was created where an inner GSS search, within the branch location loop, searched for the best match % location value. However, the results indicated that although accurate branch location and fault impedances were identified, the location % results were not close or even consistent. This is exemplified in Table 6.1. The same 7-bus radial case was utilized as before, with the branches defined between buses for a total of 6 branches.

To investigate the method's inability to identify the % location, contour plots were created to observe the change in the cost function, $L1$-norm, as % location and branch were varied with fault impedance fixed. These plots are shown in Figures 6.1-6.5.

As illustrated by the contour plots, it seems that the error norm results are not sensitive to the variation in % location. The error is low for all

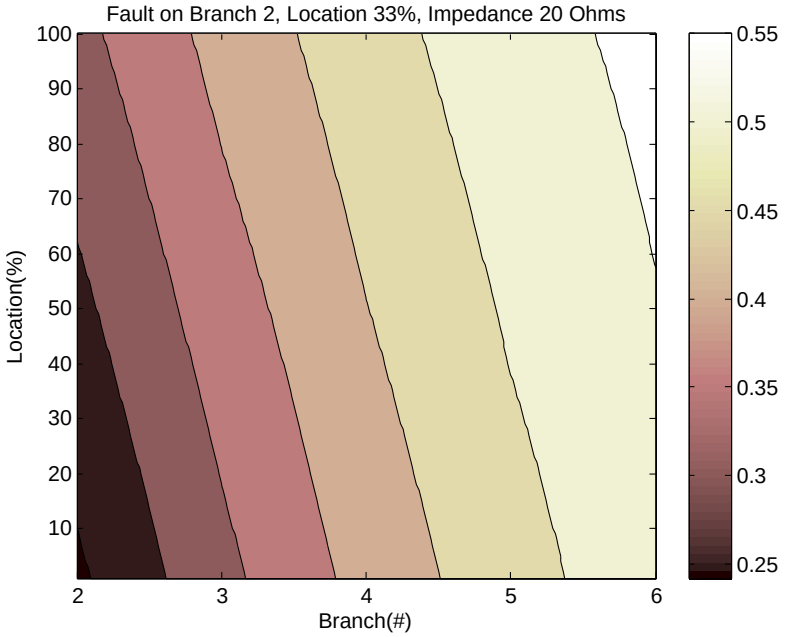

Figure 6.1: Simulated balanced three-phase fault on Branch 2, 33% Location, with Impedance 20 Ω compared with measured voltage profiles of every branch and % location combination.

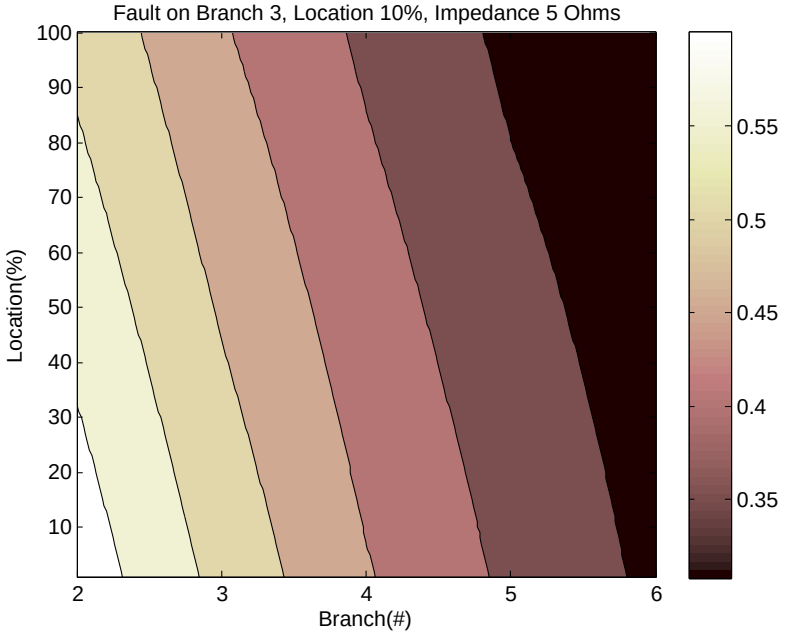

Figure 6.2: Simulated balanced three-phase fault on Branch 3, 10% Location, with Impedance 5 Ω compared with measured voltage profiles of every branch and % location combination.

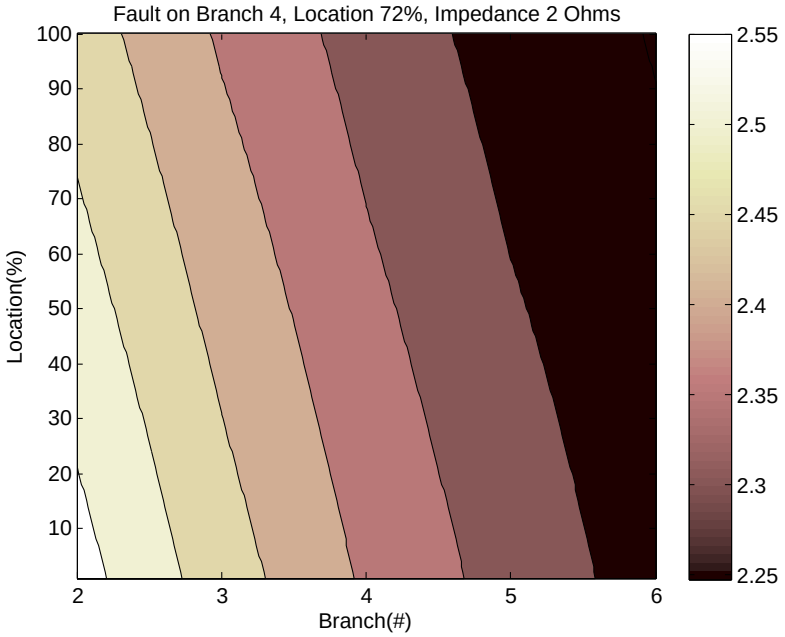

Figure 6.3: Simulated balanced three-phase fault on Branch 4, 72% Location, with Impedance 2 Ω compared with measured voltage profiles of every branch and % location combination.

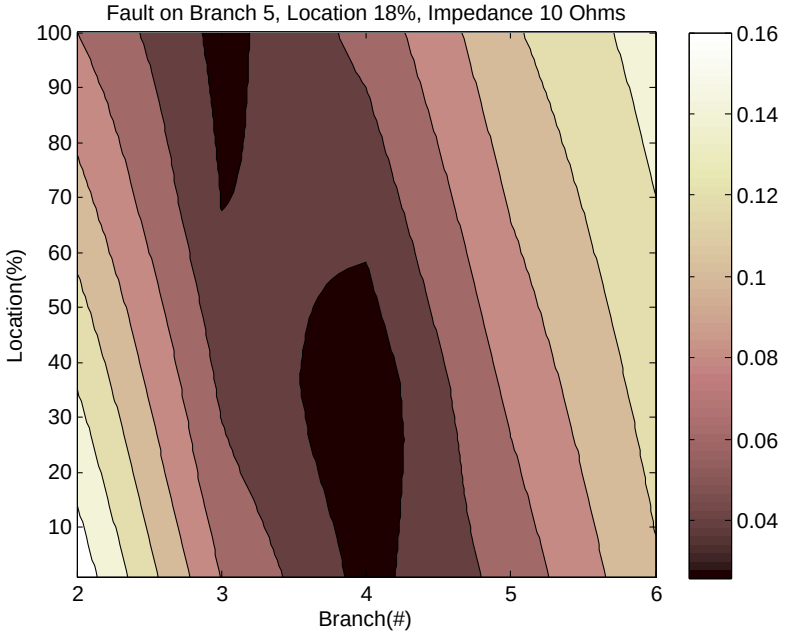

Figure 6.4: Simulated balanced three-phase fault on Branch 5, 18% Location, with Impedance 10 Ω compared with measured voltage profiles of every branch and % location combination.

Table 6.1: Results of algorithm finding branch, % location, and fault impedance after various balanced three-phase faults have occurred in 7-bus radial system.

Actual Fault	Algorithm Result
Branch 2, 33% 20 Ω	Branch 2, 1% 20 Ω
Branch 3, 10% 5 Ω	Branch 3, 1% 5 Ω
Branch 4, 72% 2 Ω	Branch 4, 61% 2 Ω
Branch 5, 18% 10 Ω	Branch 5, 62% 10 Ω
Branch 6, 20% 9 Ω	Branch 6, 99% 9 Ω

values of % location. The discontinuities in Figure 6.2 and Figure 6.4 occur because the 100% location is viewed as the next branch location. As an initial reaction, it seems to imply that perhaps the voltage profile is not affected by the minor changes in location, such as *where* along the line it occurred, but only the line itself. However, this could also be attributed to not enough measurements – that more distributed voltage monitoring devices are needed. Therefore, to acquire more measurements from the system, the case study must be altered or different simulation softwares must be explored. If the voltage profile is not sensitive to the % location variations, an alternative is to study the frequency also collected by the monitoring devices and observe if it is affected.

In an effort to increase the automation of the method, it is also a future goal to be able to detect the fault type and fault phase without user input. By incorporating these fault characteristics into algorithm, the only input would be the fact that a fault has occurred. Therefore, if the % location can be pinpointed and the fault phase and type detected, the method would be visualized as shown in Figure 6.6.

The Golden section search was the selected search technique for the minimum difference between voltage profiles for this research. However, it was initially chosen due to its straightforward implementation and guaranteed convergence. In the continuation of this work, other search techniques or comparison tools will be studied to improve the algorithm. Two related search techniques are the Fibonacci and Binary searches. In the Binary search, the method probes halfway in the interval and iteratively divides the range until the "key" is found. It requires $\log_2(N) + 1$ iterations where N is the number of elements. However, a slightly faster search that is a variant of the GSS is the Fibonacci search. This algorithm is also a divide and conquer

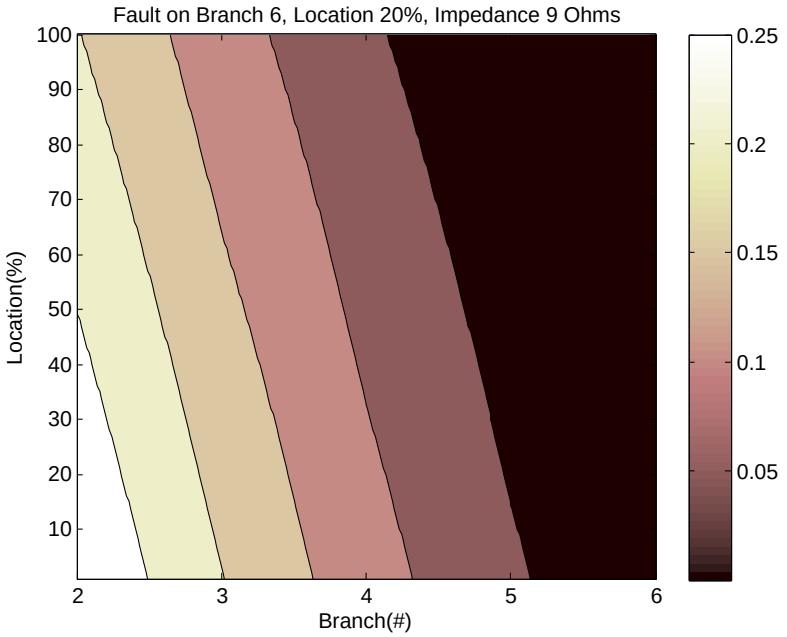

Figure 6.5: Simulated balanced three-phase fault on Branch 6, 20% Location, with Impedance 9 Ω compared with measured voltage profiles of every branch and % location combination.

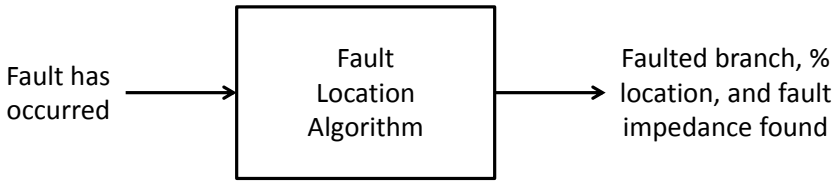

Figure 6.6: The final output of the algorithm is the faulted branch, % location, and the associated fault impedance.

algorithm that narrows down the possible locations using Fibonacci serach. Thus, it is very similar to the GSS with the difference between using the golden ratio and the Fibonacci sequence.

Powell's method is another option for finding a local minimum. It is a conjugate direction method in which the function is minimized by a bi-directional search along each search vector. It requires that the function is a real-valued function of a fixed number of real-valued inputs, though it does not need to be differentiable as no derivatives are taken. The user defines an initial point and an initial set of search vectors which are typically the normal vectors aligned to each axis. After the bi-directional search along these vectors, new positions are expressed as a linear combination of the search vectors. The method iterates until no significant improvement is made. This process can be visually interpreted in Figure 6.7.

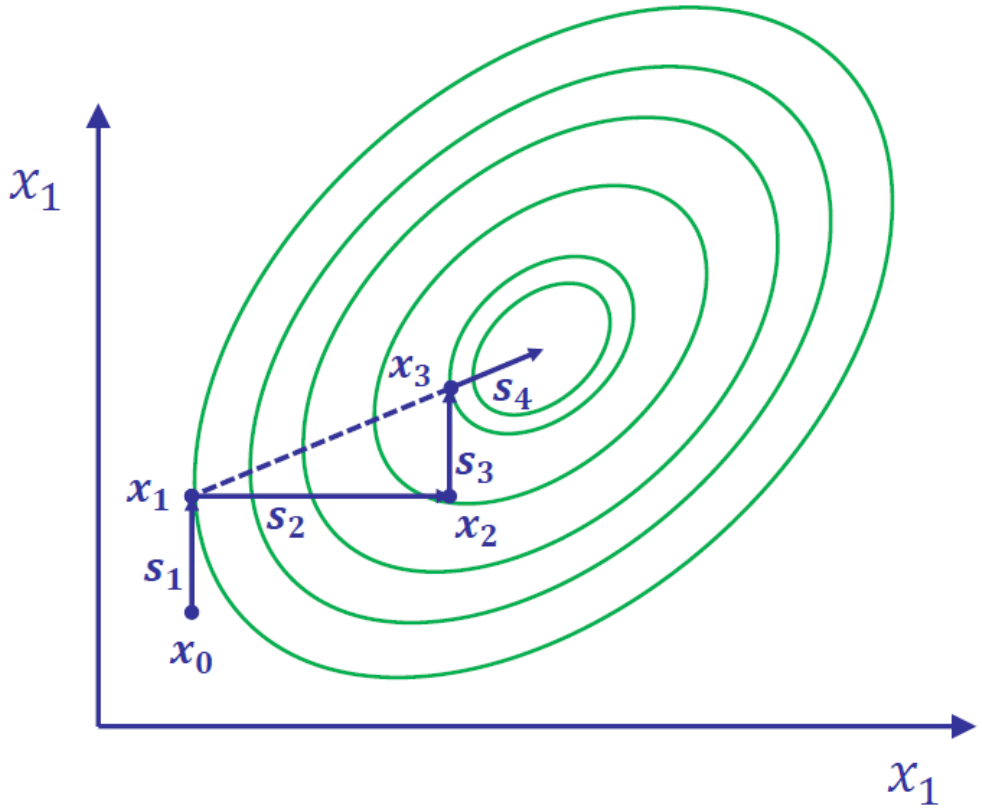

Figure 6.7: In this example, s_4 is the first conjugate search direction [6].

The method demonstrates quadratic convergence, and this desirable characteristic coupled with its lack of derivatives makes it a appealing choice for future improvements to the fault location algorithm. All in all, it is desired

that the fault location algorithm based on distributed voltage magnitude measurements is made as accurate and automated as possible. Future work for this research will be in reducing variation in results, greater search efficiency, identifying more exact locations, and detecting fault characteristics.

CHAPTER 7

CONCLUSION

Distributed voltage monitoring devices are a result of an effort to increase situational awareness, an integral part of the smart grid initiative. Fault location is a critical component of the reliability and efficient functioning of the power grid. There have been many location algorithms developed for transmission systems, but there exists a lack in the domain of the distribution systems. It is often difficult to translate a method designed for a transmission system to that of distribution due to lack of instrumentation and line complexity. This can be remedied with the advent of distributed voltage monitoring devices, allowing for voltage information to be collected throughout the distribution network.

With this newfound availability of extensive, fast-sampled voltage magnitude data, a fault location algorithm using only the voltage information can be developed. After a fault occurs, the characteristic voltage profile, or voltage sags, can be studied to locate the fault. Nonetheless, previous methods focusing on voltage sags still require current measurements. With the distributed devices, it is possible to use only the voltage information provided. Such a method will simplify the implementation and also take full advantage of the economical distributed voltage monitoring device capabilities.

The proposed algorithm intelligently compares measured and simulated voltage profiles to obtain the best match fault location. The simulated locations are selected using the Golden section search and compared against the measured voltage profile using the $L1$-norm as a cost function. By searching for the fault location and fault impedance that outputs the lowest norm error, the most likely combination is found. The algorithm is further streamlined with the use of an automation server to create an interface between power system simulation and computational softwares – automating the transfer and storage of data between the two platforms. The results indicate that the method worked successfully, with close accuracy and few iterations.

Presently, the algorithm can pinpoint which bus and with what impedance the fault was incurred, given the fault type and phase. In the future, it is to be explored if a more exact location, such as % along the line can be identified and if the fault type and phase can be detected automatically. The method will also continued to be improved to reduce impedance variation and achieve greater accuracy.

REFERENCES

[1] S. Lotfifard, M. Kezunovic, and M. Mousavi, "Voltage sag data utilization for distribution fault location," *Power Delivery, IEEE Transactions on*, vol. 26, no. 2, pp. 1239–1246, 2011.

[2] H. Li, A. S. Mokhar, and N. Jenkins, "Automatic fault location on distribution network using voltage sags measurements," in *18th International Conference on Electricity Distribution*, The University of Manchester, United Kingdom. CIRED, 2005.

[3] Z. Galijasevic and A. Abur, "Fault location using voltage measurements," *Power Delivery, IEEE Transactions on*, vol. 17, no. 2, pp. 441–445, 2002.

[4] J. D. Glover, "Electric power distribution," in *Encylopedia of Energy Technology and The Environment*. John Wiley and Sons, 1995.

[5] R. E. Shatshat, "Ele b7 power systems engineering: Balanced (symmetrical) faults," Unpublished, 2009.

[6] B. German, "Unconstrained optimization: Line search algorithms, ae 8803 ger: Optimization for the design of engineered systems," Unpublished, 2013.

[7] P. Dutta and M. Kezunovic, "Fault resistance sensitivity of sparse measurement based transmission line fault location," in *North American Power Symposium (NAPS), 2011*, Aug 2011, pp. 1–7.

[8] D. Hou, "Detection of high-impedance faults in power distribution systems," in *Power Systems Conference: Advanced Metering, Protection, Control, Communication, and Distributed Resources, 2007. PSC 2007*, March 2007, pp. 85–95.

[9] M. Kezunovic, "Optimized fault location," Power Systems Engineering Research Center, Concurrent Technologies Corporation Final Project Report, April 2008.

[10] J. D. Glover, M. S. Sarma, and T. J. Overbye, *Power System Analysis and Design*, 5th ed. Cengage Learning, 2012.

[11] L. Renforth, R. Mackinlay, and M. Seltzer-Grant, "Deployment of distribution on-line partial discharge monitoring devices on medium voltage electricity networks," in *Electricity Distribution - Part 1, 2009. CIRED 2009. 20th International Conference and Exhibition on*, June 2009, pp. 1–4.

[12] M. Gilger, "Addressing information display weaknesses for situational awareness," in *Military Communications Conference, 2006. MILCOM 2006. IEEE*, Oct 2006, pp. 1–7.

[13] F. C. L. Trindade, W. Freitas, and J. C. M. Vieira, "Fault location in distribution systems based on smart feedermeters," *IEEE TRANSACTIONS ON POWER DELIVERY*, pp. 251–260, February 2014.

[14] "Fundamentals of electricity: Radial, loop, & network systems," Electric Power Board, Tech. Rep. [Online]. Available: http://epb.apogee.net/foe/ftdstr.asp

[15] S. Hanninen and M. Lehtonen, "Characteristics of earth faults in electrical distribution networks with high impedance earthing," *Electric Power Systems Research*, vol. 44, no. 3, pp. 155 – 161, 1998.

[16] D. P. Bertsekas, *Nonlinear Programming*, 2nd ed. Athena Scientific, September 1999.

[17] S. Hossain, H. Zhu, and T. Overbye, "Distribution fault location using wide-area voltage magnitude measurements," in *North American Power Symposium*. IEEE, September 2013.

[18] *PowerWorld Web Help Manual*, PowerWorld Corporation, Champaign, IL, October 2013. [Online]. Available: http://www.powerworld.com/WebHelp/Default.htm

[19] B. Rector, "Introducing longhorn for developers," October 2003. [Online]. Available: http://msdn.microsoft.com/en-us/library/aa479874.aspx

[20] *Auxiliary File Format for Simulator 17*, PowerWorld Corporation, Champaign, IL, July 2013.

[21] S. Hossain, S. Mohapatra, T. J. Overbye, and C. Marzinzik, "Automation of commercial power system software for data-driven research," in *Power and Energy Conference 2014*, February 2014.